Interface Heat Transfer in Investment Casting of Aluminum Alloys

DAVID J. BROWNE and DENIS O'MAHONEY

Via design of experiments and using a newly developed inverse method, the heat-transfer boundary conditions in the investment casting process have been studied. It has been shown in the past that these conditions, expressed as interface heat transfer coefficients (HTCs), vary during alloy solidification and cooling. In this work, the authors have studied the additional effects of alloy solidification range, metallostatic head, investment shell thickness, preheat, and interface geometry. This provides an improved set of relationships from which to build realistic boundary conditions into computer simulations of shape casting. Using axisymmetric solidification experiments and numerical inverse analysis, it is shown that the effect of metallostatic head is only significant for long freezing-range alloys. Increasing shell mold thickness and preheat also have effects that are alloy-dependent, and significant differences in thermal behavior are reported between the alloy/mold interface and the alloy/core interface. The four alloys used in the experiments are aluminum-based and vary from short freezing-range commercially pure to an alloy with a freezing range of 120 °C.

I. INTRODUCTION

WHEN liquid metal spreads over a solid surface, a perfect thermal contact cannot be achieved. This is a result of such factors as roughness of the solid surface, the surface tension of the melt, impurities on the surface, and gas entrapment. If the surface temperature is below the liquidus of the metal alloy, then after the alloy has partially solidified, other factors that influence the thermal contact include interface geometry and the pressure applied to the solidifying metal. The nature of the thermal contact between solidifying metal and mold is characterized by a heat transfer coefficient (HTC), the determination of which is often achieved by inverse techniques. It is critical for the proper numerical modeling of solidification that this boundary condition is known accurately. The interface HTC (h_{int}) is given by

$$h_{\text{int}} = \frac{q_{\text{int}}}{\Delta T_{\text{int}}} \quad [1]$$

Here, ΔT_{int} is the temperature drop across the interface, and q_{int} the interfacial heat flux per unit area. In general, h_{int} is not constant but varies during solidification and depends upon a number of factors.[1]

For a given mold, the main variable to consider in interface heat transfer analysis is the alloy composition. This determines such factors as surface tension (of the liquid) and freezing range, both of which can have a significant effect on the interface heat transfer.[2] As the surface tension increases, the alloy will be less able to conform to the shape of the mold, thus reducing the effective contact area and increasing the resistance to heat flow. Alloys with a short freezing range will form a well-defined solid shell at the outer surface and may tend to contract away from the interface. This will reduce the contact pressure and the HTC. As the freezing range increases, the alloy will tend to solidify in a less directional manner.

Increasing the depth to which the alloy is poured increases the pressure of the liquid metal at the interface, helping to overcome surface-tension forces. It may also help the alloy to resist thermal contraction of the solid shell next to the interface, thus maintaining good thermal contact.

The pouring temperature for most aluminum alloys is typically 700 °C. Above this temperature there is a risk of burning off some of the alloying elements (Mg in particular). The amount of shrinkage and the solidification time also increase with pouring temperature. Low initial superheat can lead to incomplete filling. Thus, there is little to be gained by altering the pouring temperature. For aluminum investment casting, the mold preheat is usually between 300 °C and 500 °C. Increasing preheat reduces the amount of heat a mold can absorb, the thermal gradient across the mold, and the amount by which it will expand when heated.

Varying the mold thickness affects the ability of the mold to absorb heat from the metal and its ability to expand when heated. Prabhu *et al.*[1] examined the solidification of an aluminum alloy in a cylindrical-steel mold. It was found that the interface HTC increased as the mold wall thickness decreased. Michael *et al.*[3] also studied the solidification of various aluminum alloys in a cylindrical steel mold. It was noted that heating the mold slightly (to about 150 °C) increased the maximum interface HTC. This was explained by the fact that a cold mold will favor surface solidification, which will reduce the heat-transfer rate thereafter.

The behavior of the alloy/core interface has been previously studied in permanent molds.[4,5,6] A significant difference between short and long freezing-range alloys was observed. Kim and Lee[4] studied the solidification of several aluminum alloys around a cylindrical steel core in a cylindrical steel mold. The alloys were pure aluminum, A390, and A356. For the long freezing-range alloy A356 the HTC fell from 2000 W/m^2 K to about 500 W/m^2 K, then rose again as solidification was nearing completion, and continued to rise afterwards. While for the short freezing-range alloys, which tend to form shells on solidification, the HTC rose

DAVID J. BROWNE, Lecturer, is with the Department of Mechanical Engineering, University College Dublin, Dublin 4, Ireland. DENIS O'MAHONEY, Research Scientist, is with the National Microelectronics Research Centre, University College Cork, Cork, Ireland.

Manuscript submitted February 6, 2001.

rapidly during and after solidification. The reason given for this is that the short freezing-range alloys form a coherent shell around the core and contract onto it, thus increasing the contact pressure and contact area. While the long freezing-range alloys do not form a coherent structure until they are about 50 pct solidified. It is at this point that the HTC rises.

Information available on interface HTCs for the investment casting process is meager. An early estimation of the interface HTC for an aluminum-alloy (A356) investment casting was published by Sturm and Sahm.[7] The casting considered was an aerospace structural component. The HTC was assumed to be constant, and the value determined was 1000 W/m^2 K.

Anderson *et al.*[8] carried out a combined simulation/experimental program to study the thermal behavior of a two-dimensional, symmetrical aluminum investment casting. The interface HTC was buried in an overall HTC. Values for the alloy/mold interface HTC were not reported.

Sahai and Overfelt[9] completed a study of interface HTCs for a nickel-based alloy (INCONEL* 718) for cylindrical and plate investment castings. For the cylindrical casting (mold preheat of 745 °C), the interface HTC varies in a linear fashion from 200 W/m^2 K at a metal temperature of 1300 °C to 100 W/m^2 K at 850 °C. For the plate casting, the HTC was found to vary between 5000 W/m^2 K at 1400 °C to 100 W/m^2 K at 1100 °C. The gap between the alloy and the mold was measured using X-ray methods. It was of the order of 1 mm but increased slightly from bottom to top of the casting.

*INCONEL is a trademark of INCO Alloys International, Huntington, WV.

Despite the output of previous work, it is difficult, when setting up a computer simulation of investment casting, to assign boundary conditions appropriate to the real casting situation. This is because these conditions vary not only with time, but also with temperature (or alloy solid fraction), alloy type, geometry, and metallostatic head. Other variables requiring consideration include shell preheat and thickness. So here the authors investigate the effects of key casting parameters on interface heat transfer. Factorial designed experiments are used to increase the efficiency of the investigation.

II. NUMERICAL METHOD

An inverse heat conduction problem is one where interior temperature measurements of a body are used to obtain the surface heat flux and surface temperature. Using this information, interface HTCs can be determined (Eq. [1]).

Inverse heat transfer problems are more difficult to solve than classical direct problems where boundary conditions are known. This is because errors in measured data are amplified as these measurements are projected to the surface. Inverse methods are employed to find boundary conditions since the presence of a temperature sensor at a boundary may impair the accuracy of such a measurement. It may be impossible to locate a sensor accurately at a boundary, or indeed the boundary may be simply inaccessible.

The method by which the interface HTCs are determined using thermal data recorded during the solidification of aluminum alloys is described elsewhere.[10,11] The method used has been shown to be accurate and reasonably insensitive to noise in measured data. It has also been shown to compare well with other inverse methods, particularly when phase change problems are considered.

III. EXPERIMENTAL

A. *Material Thermal Properties*

The approach to calculating HTCs employed in this work requires knowledge of the thermal properties of the investment shell materials and the aluminum alloys used in the experiments. The relevant properties of aluminum and its alloys are widely available in the literature.[12] The method by which the solid fraction evolution of an alloy was determined in this work is based on techniques described elsewhere.[13] There is relatively little accurate information available on the thermophysical properties of the ceramic materials used to manufacture investment casting shell molds. Investment shell molds are usually composed of two layers. The primary layer is generally zircon, which is used because it gives good surface finish and is resistant to thermal shock. The secondary layer of alumino-silicate is used for strength. Although this combination of ceramic materials is often used in industry, other investment shell compositions have also been used successfully in practice. It is beyond the scope of this work to investigate all shell systems in common use, but it is believed that the broad thrust of the findings presented here is generally applicable, although it is expected that actual numerical values obtained for HTCs will vary between systems.

A number of tests were carried out on these materials in order to determine their thermal properties. These are described elsewhere.[10,11,14] For zircon, the variation with temperature of specific heat capacity is very weak and is approximately 800 J/kg K at 400 °C. For the alumino-silicate material, the specific heat capacity is found to vary in a linear fashion from 1020 J/kg K at 300 °C to 1140 J/kg K at 700 °C. The thermal conductivity of zircon was found to be approximately 2 W/m K, and the effect of temperature in the range 400 °C to 700 °C was found to be very weak. The thermal conductivity of alumino-silicate in the region 400 °C to 700 °C was found to be approximately constant with a value of 0.75 W/m K.

The mold/atmosphere HTC combines the effects of convective and radiative modes of heat transfer at the outer mold surface. This is determined by experiment and inverse analysis. Details are presented in Appendix A. For alumino-silicate, the mold surface HTC at 300 °C is 22 W/m^2 K and rises to 34 W/m^2 K at 600 °C. The increase is partially due to the incorporation in the measured value of increased radiative effects.

B. *The Alloy/Mold Heat-Transfer Coefficient (h_{int})*

The effects of casting variables, such as alloy, metallostatic pressure, and mold preheat on the interface HTC are difficult to gage *ad hoc*. Previous attempts to quantify these effects have usually been carried out in a "one change at a time" fashion. With a large number of variables to consider, this could lead to a substantial amount of experimentation in order to determine the dominant variables.

An alternative approach, based on the methods described

Table I. General Experimental Schedule

Experiment	Fac1	Fac2	Fac3	Op
1	−	−	−	Op1
2	+	−	+	Op2
3	−	+	+	Op3
4	+	+	−	Op4

Table II. Experimental Schedule for Molds of 15 mm Thickness

Experiment	Mold Preheat (°C)	Head (d) (cm)	Primary Layer Thickness (mm)
1	300	8	3
2	500	12	3
3	300	12	1
4	500	8	1

by Grove and Davis,[15] is to use statistically designed experiments. In each experiment, the value of more than one variable is changed. Usually, a variable (or factor) has two values, a maximum (+) and minimum (−). The experimental schedule used in this study is based on Table I. Here, Fac1, Fac2, and Fac3, are arbitrary variables, and Op is the measured output (HTC, say).

In order to assess the effect on the output caused by changing a variable, the average value of the output when the variable is a maximum is compared to that when it is a minimum. So for example, the effect of Fac1 on the output is found by comparing the average of Op2 and Op4 to that of Op1 and Op3 (*i.e.*, the average value at Fac1+ is compared to the average value at Fac1−). This is repeated for all variables of interest. Hence, the principal variables can be obtained.

The variables that were altered to assess their influence on the HTC at the metal/mold interface (for a given aluminum alloy and mold thickness) are mold preheat, metallostatic pressure, and primary layer thickness. For a given mold, varying the primary layer thickness changes the thermal resistance of the mold and its capacity to transmit heat. This is because the primary and secondary layers have different thermal properties. As the primary layer forms the interface surface and a significant part of the mold, it is reasonable to check whether or not changing its thickness affects the thermal behavior of the interface. The effect of geometry will be considered separately. The schedule of experiments for these alloys is shown in Tables II and III and is based on Table I. The two tables should be considered separately. The aluminum alloys considered in this study are 413, A356, and 319 (Aluminum Association designations). The freezing range data for these alloys are given in Table IV.

The test piece used (Figure 1) is a cylindrical mold with two thermocouples, one in the mold cavity (T1) and one in the mold wall (T2). A detailed description of the preparation of the experiment is presented in Reference 11 and in summary form in Appendix B. When the alloy is poured, the thermal history at both points is recorded. The sensing tips of the thermocouples are both located a distance, d (which represents the metallostatic head) beneath the initially liquid-free surface. Values for d of 8 and 12 cm do not represent the complete range of possible casting configurations in

Table III. Experimental Schedule for Molds of 20 mm Thickness

Experiment	Mold Preheat (°C)	Head (d) (cm)	Primary Layer Thickness (mm)
5	300	12	7
6	500	8	7
7	300	8	5
8	500	12	5

Table IV. Thermal Data for Aluminum Alloys Used[10]

Alloy	Liquidus Temperature (°C)	Eutectic Temperature (°C)	Solidification Completion Temperature (°C)	Freezing Range (°C)
413	579	577	575	4
A356	612	570	548	64
319	610	561	490	120

industry, but they are chosen subject to the constraints of (a) being sufficiently different from one another, while (b) being far from either the top or bottom of the casting to avoid end effects, thereby enabling a one-dimensional (radial) analysis of the heat flow. Additional insulation at both top and bottom of the casting also helps in this regard (Appendix B). To determine the interface HTC, four calculations need to be performed.

First, the thermal history between the mold surface and T2 is found. This is a direct problem as the mold/atmosphere HTC is known. Next, the thermal history between the center of the alloy and T1 is found. This is a direct problem as the center of the alloy is an adiabatic boundary. Then, the two inverse problems between T1 and the alloy surface, and T2 and the mold surface are solved. The alloy/mold HTC can now be found *via* Eq. [1], as the interface temperature drop and heat flux are known.

C. *The Alloy/Core Heat-Transfer Coefficient (h_{cor})*

The test piece for the alloy/core experiments is shown in Figure 2. It is composed of a hollow outer (cylindrical) mold and an interior core, which are made separately and then joined together at the base and top. Two thermocouples are used. The first (T1) is placed in the core near its surface, the second (T2) is placed in the mold cavity near the core surface. Experimental details are similar to those used in determination of the other HTCs (Appendices). The alloy is poured, and the thermal history at both points recorded. To determine the interface HTC, four calculations need to be performed.

First, the thermal history between the center of the core and T1 is found. This is a direct problem as the center of the core is an adiabatic boundary. Next, the direct problem in the alloy is solved, as the alloy surface heat flux into the mold has already been calculated, as described in Section III–B. Then, the two inverse problems between T2 and the alloy surface, and T1 and the core surface are solved. The core/alloy HTC (h_{cor}) can now be found, as the interface temperature drop and heat flux are known.

For pure aluminum, 413, A356, and 319, h_{cor} as a function

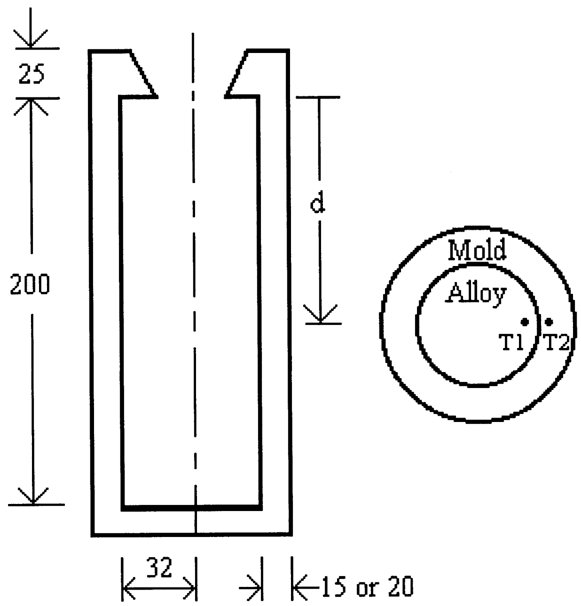

Fig. 1—Schematic of test for alloy/mold interface HTC estimation; distance *d* represents the metallostatic head (dimensions in millimeters).

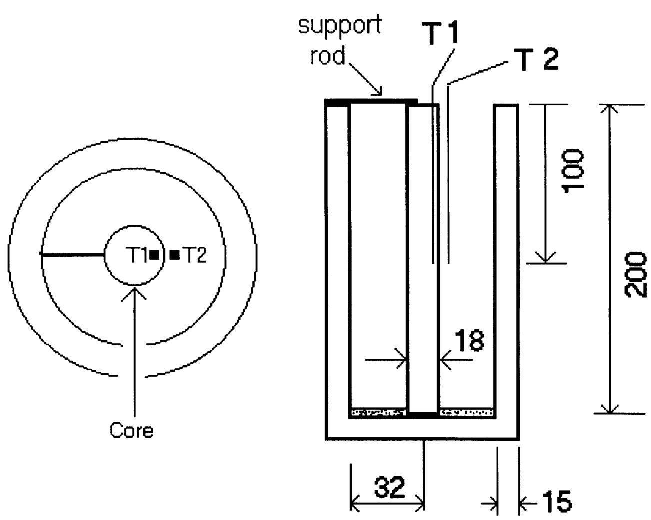

Fig. 2—Schematic of test for alloy/core interface HTC estimation (dimensions in millimeters).

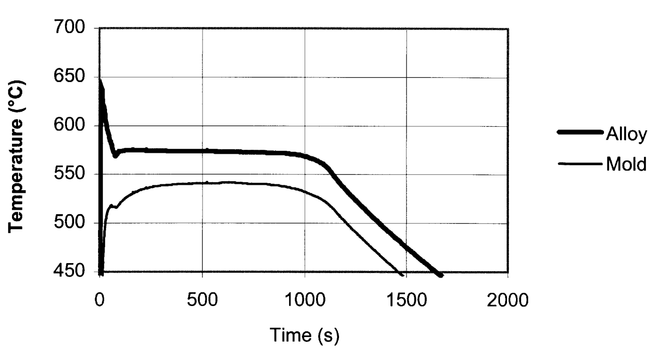

Fig. 3—Cooling curves for experiment 1—alloy 413.

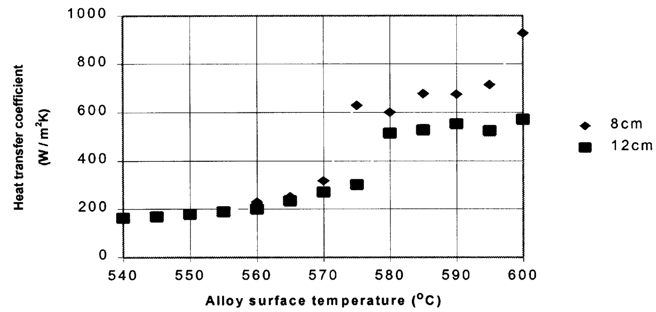

Fig. 4—Alloy 413: HTCs in a 15 mm mold preheated to 300 °C, for d = 8 cm (experiment 1), and d = 12 cm (experiment 3).

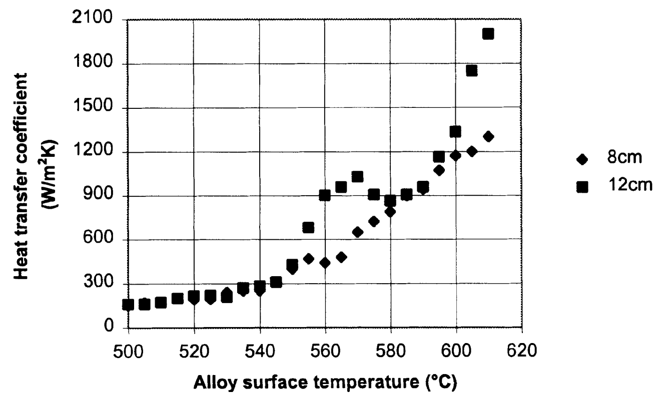

Fig. 5—A356: HTCs in a 15 mm mold preheated to 300 °C, for d = 8 cm (experiment 1) and d = 12 cm (experiment 3).

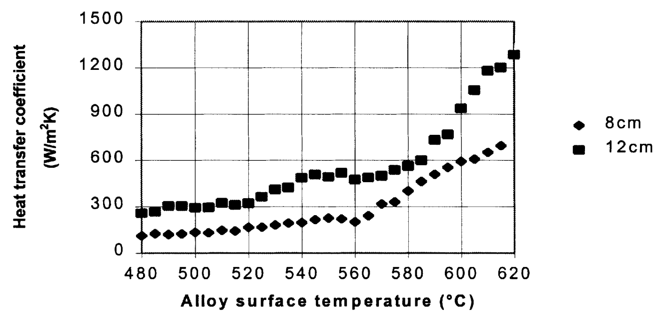

Fig. 6—Alloy 319: HTCs in a 15 mm mold preheated to 300 °C, for d = 8 cm (experiment 1) and d = 12 cm (experiment 3).

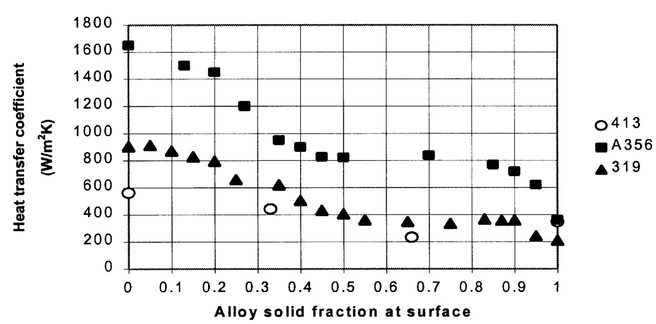

Fig. 7—HTC variation for 15 mm mold, 300 °C preheat.

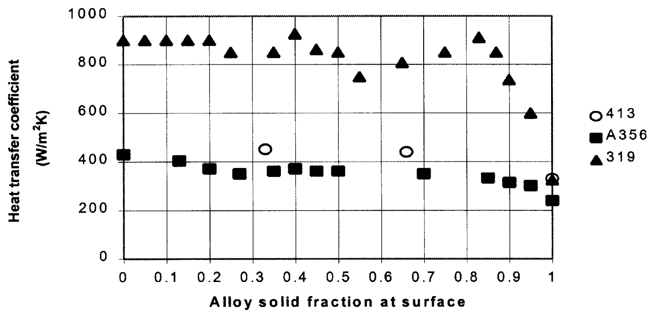

Fig. 8—HTC variation for 15 mm mold, 500 °C preheat.

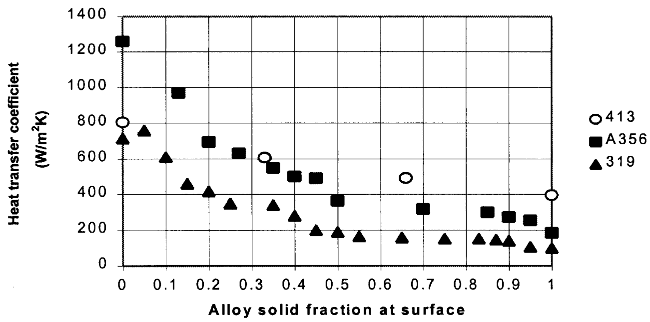

Fig. 9—HTC variation for 20-mm mold, 300 °C preheat.

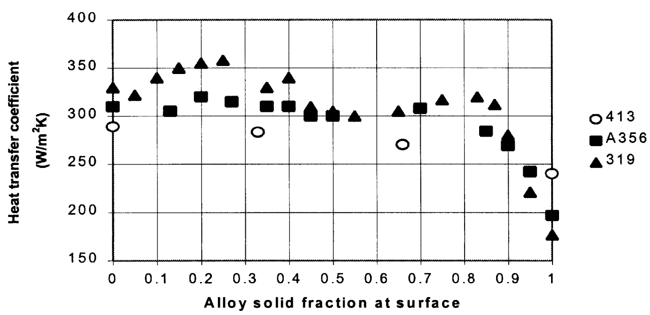

Fig. 10—HTC variation for 20-mm mold, 500 °C preheat.

of alloy surface temperature is determined. In all cases, the mold preheat temperature is 400 °C, the alloy is poured at 700 °C, and the thermocouple depth is 10 cm. Each experiment is performed twice.

IV. RESULTS AND DISCUSSION

Figure 3 shows a typical cooling curve for alloy 413 (experiment 1). Figures 4, 5, and 6 show the variation in computed HTC for alloys 413, A356, and 319, respectively, as a function of alloy surface temperature (experiments 1 and 3).

Figures 7 through 10 show the dependence of interface HTC on alloy solid fraction at the alloy/mold surface for different combinations of mold preheat and thickness. The graphs are prepared by taking the average of the HTC at the two heads (8 and 12 cm), which is then converted into a HTC based on alloy solid fraction.[10,11] The overall average

Table V. Average Values of h_{int} (W/m^2 K) for 15 mm Mold

	Alloy			
Preheat	413	A356	319	Average
300 °C	391	975	550	640
500 °C	425	320	820	521

Table VI. Average Values of h_{int} (W/m^2 K) for 20 mm Mold

	Alloy			
Preheat	413	A356	319	Average
300 °C	609	575	325	503
500 °C	275	290	309	291

Table VII. Average Value of h_{int} (W/m^2 K) Based on Mold Thickness

	Mold Thickness		
Alloy	15 mm	20 mm	Average
413	408	442	425
A356	650	430	540
319	685	330	500
Average	581	400	482

values of the HTC are then calculated; they are shown in Tables V, VI, and VII.

Figure 4 shows the evolution of interface HTC for the short freezing-range alloy 413. It can be seen that the effect of the head is not a significant factor.[10,11] Figure 5 shows the variation of interface HTC for alloy A356. A reduction in HTC is obvious at around 570 °C. This is probably due to the rapid increase in solid fraction between 571 °C and 570 °C.[10] This leads to the development of a coherent shell of solid that may have sufficient strength to pull away from the mold wall. Within the solidification range, however, the higher level of metallostatic head is seen to lead to more efficient transfer of heat from the A356 alloy to the mold. Figure 6 shows the variation of interface HTC for alloy 319. It can be seen that higher values of head produce higher HTCs. It should be noted that the effect of head is greater than that for alloy 413, which has a much shorter freezing range.

At low mold preheat, a large variation of the HTC across the freezing range is observed (Figures 7 and 9). This is because initial rates of heat flux are high due to the large difference in temperature between the alloy and mold. As solidification progresses, the heat flux diminishes, and the temperature drop across the interface increases further; this leads to a drop in calculated HTC. The high rate of heat transfer will also cause the mold to expand, the relative expansion being large when the initial mold temperature is low. At the same time, the casting will start to solidify and contract leading to a drop in contact pressure and, hence, in HTC.

For a high mold preheat, the results show a lower variation of HTC across the freezing range (Figures 8 and 10). Here, the mold will not expand as much as for lower preheat, allowing it to stay in closer contact with the casting. The heat flux is also low (because of the initial gradient) and varies less during solidification, leading to a smaller variation in HTC. However, alloys A356 and 319 show a very sudden decrease in HTC when the solid fraction rises to about 0.85.

Tables V and VI show the value of the average HTC for the 15 and 20 mm molds respectively, at both 300 °C and 500 °C preheat. Table VII shows the overall average of the HTC based on mold thickness only. Mold preheat is seen to be a more significant factor than thickness, indicating that the ability of the mold to absorb heat is more dependent on its temperature than size. The use of thicker molds leads to a modest reduction (about 30 pct) in the HTC. The difference in temperature between the inner and outer surfaces of the mold increases with thickness. The outside mold surface temperature does not rise as high as for the thinner mold. Also, strength increases with increasing thickness. Thus, thicker molds expand less when heated and are able to resist contraction on cooling, making air gaps more likely to form.

On the other hand, thin molds expand more readily on initial heating, as the temperature is more uniform across the mold, and the mold wall is weaker. At this stage, the alloy is still liquid, and good thermal contact will be maintained. Thin molds also contract more readily on cooling. Thus, good thermal contact is maintained during solidification, which yields a higher average value of HTC than with thick molds.

Figures 4 to 6 show the effects of metallostatic head for molds preheated to 300 °C. On the other hand, results for 500 °C preheat (Figures 8 and 10) are averages of the values computed for low and high metallostatic heads. But the authors have noted that, for the medium freezing-range A356 and even more so for the long freezing-range alloy 319, the effect of head is much greater at higher preheat, experiments 2 and 4. This can be verified by comparing Figures 5 and 6 to Figures 10(b) and (c) of Reference 11, respectively. At high mold preheat, there are low temperature gradients in the casting, so for long freezing-range alloys, the entire casting is at, or nearly at, the fraction solid of the interface. So there is no solid outer shell. The effect of head is greater when acting through a mush than when acting through liquid on a shell of near-solid. This would also go to explaining the reversal of the relative positions of alloys 319 and A356 from Figures 7 to 8 (from low to high preheat): mushy alloys, such as 319, are at an advantage, in terms of maintenance of thermal contact with the mold, over alloys with shorter freezing range at high mold temperature.

Contrary to expectations, primary layer thickness was not found to have a very significant effect on interface heat transfer in investment casting. For the 15 mm mold, a reduction in primary layer thickness (from 3 to 1 mm) results in an average reduction of 16 pct in the HTC. For the 20-mm mold, the thinner primary layer produces an increase of 3 pct in HTC.

Figures 11 through 14 show the variation of alloy/core HTC for pure aluminum, alloy 413, A356, and 319, respectively. The maximum value in all cases is about 1000 W/m^2 K. For the longer freezing-range alloys, the HTC tends to rise during solidification, and after it is complete. For alloys A356 and 319, there is a slow increase in the HTC as solidification progresses; this agrees with Kim and Lee[4] for long freezing alloys.

An interesting point about heat transfer in these cores is that, once the thermal gradient reverses, the core acts as a heat retainer in the center of the casting, rather than as a heat sink. From Figures 11 through 14, alloy freezing range increases. Also, the final HTC rises.

Alloy 413 shows a decrease in HTC during solidification (Figure 12), which levels off once solidification is complete. It is worth noting here that this variation of HTC for the shell forming alloy (413) is not the same as that reported, for steel cores, by others.[4] The core is heated by the molten alloy and is quickly saturated with heat. But, as cooling is from the outer mold surface (Figure 2), a thermal gradient is

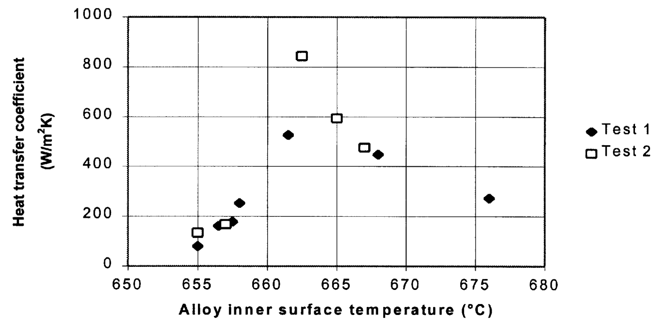

Fig. 11—Evolution of alloy/core HTC for pure Al.

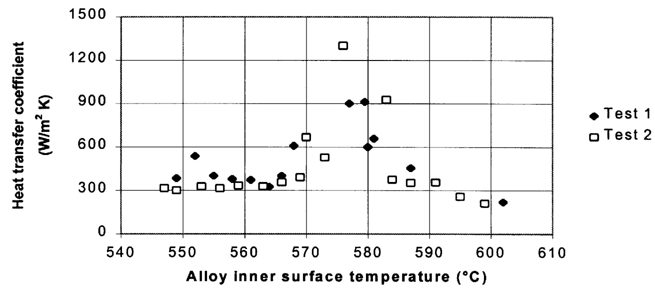

Fig. 12—Evolution of alloy/core HTC for alloy 413.

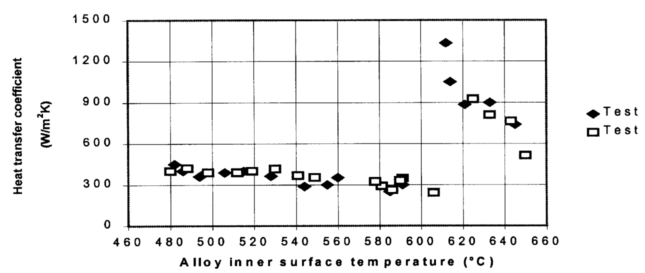

Fig. 13—Evolution of alloy/core HTC for A356.

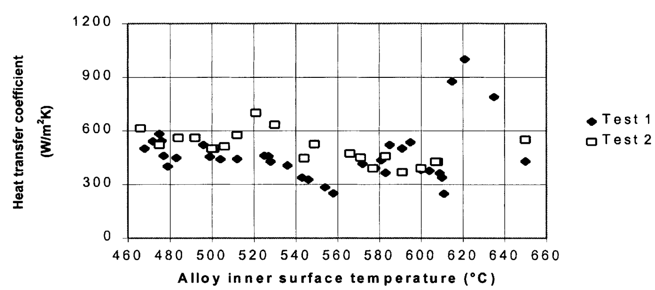

Fig. 14—Evolution of alloy/core HTC for alloy 319.

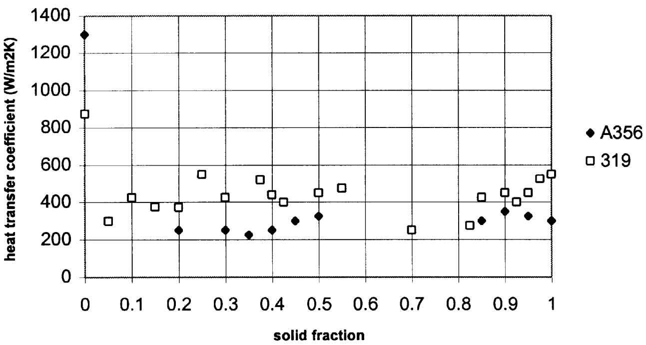

Fig. 15—Alloy/core HTC variation with alloy solid fraction.

established during alloy solidification, with the core having a higher temperature than the alloy. Thus, the material beside the core is the last to solidify. For the longer freezing-range alloys, there will be a flatter distribution of fraction solid across the alloy (from core to mold). For short freezing-range alloys, solidification will be very much more from the outside in. In this latter case, the liquid alloy may move away somewhat from the core to feed solidification shrinkage occurring further out in the casting. This concurs with observations by the authors of a deep sink in the pure aluminum casting, close to the core. Figure 15 shows the variation in alloy/core HTC as a function of alloy fraction solid near the core for alloys A356 and 319.

When large changes in solid fraction occur, thermal gradients flatten in the core leaving gaps in the HTC data. The problem of finding alloy/core HTCs is further compounded by the fact that the measured temperature drop across the interface is small (usually 2.5 °C to 4 °C). As the resolution of the temperature measurement is only ±0.5 °C and the thermocouples are guaranteed to ±1 °C, significant error is likely to arise. Indeed, Thomas[16] reported that it is almost impossible to obtain an interface temperature drop to an accuracy of greater than 0.5 °C. This would go some way to explaining the scatter in the results: there are differences between the output of the two tests performed at each experimental setting.

V. SOURCES OF ERROR AND EXPERIMENTAL UNCERTAINTY

One-dimensional models are commonly used in inverse heat-conduction calculations; this is due to the significant increase in complexity when two-dimensional models are employed. This is a significant simplification as the interface HTC shows a dependence on the initial head of liquid metal. Indeed recent work[17,18] shows that molds with low thermal conductivity tend to promote nonuniform freezing along the vertical sides of a casting.

After the mold is filled, it takes a significant length of time (about 4 seconds) for the thermocouple to come up to the temperature of the metal. This is due to the alloy freezing as it touches the thermocouple and then being remelted. Also, the presence of the alumina sheath (which protects the thermocouple, enabling its reuse, and keeps it mechanically stable) reduces the speed of response. But the sheath wall thickness is only 0.5 mm (Appendix A) and made of alumina, which has a reasonable thermal conductivity—much higher than that of the investment shell material. As such, it does

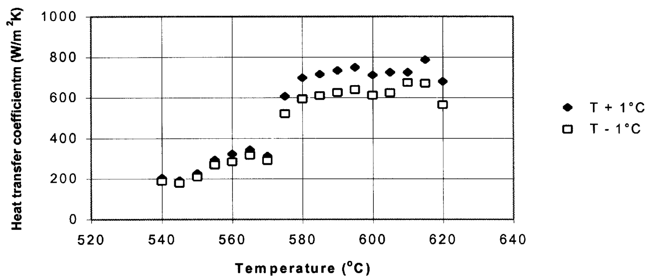

Fig. 16—Effect of mold thermocouple bias (±1 °C) on calculated HTC.

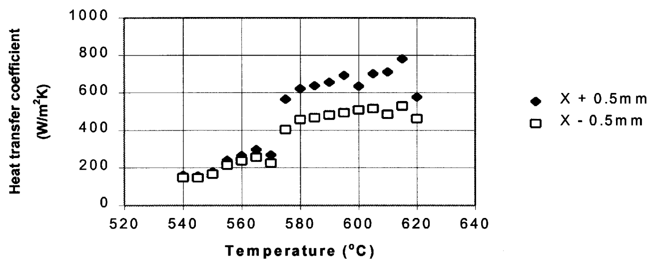

Fig. 17—Effect of uncertainty (±0.5 mm) in mold thermocouple position (X) on calculated HTC.

not constitute significant thermal insulation. Also, the calculations performed in this work are largely based on relative temperatures, so as the same sheath is used for all thermocouples, any effects of time lag, *etc.* will not adversely affect the results. Furthermore, as the time scales involved in the experiments are of the order of minutes (Figure 3), time-lag effects are not significant. The position of the thermocouples can be measured to an accuracy of ±0.5 mm. The thermocouples themselves are guaranteed to an accuracy of ±1 °C.

In order to assess the level of uncertainty associated with the calculation of interface HTCs, the following analysis was performed. A356 was cast with a mold of 15-mm thickness and a preheat temperature of 500 °C. Two thermocouples were placed 10 cm from the top in both alloy and mold, as before. Figures 16 and 17 show the variation of calculated interface HTC when the mold thermocouple bias and mold thermocouple position are artificially varied. It can be seen that uncertainties in the bias of the thermocouple and in the thermocouple position influence the calculation. It has been shown that uncertainties in mold thickness and thermal diffusivity are less important.[11] Owen[19] reported that HTCs are very sensitive to the bias of the thermocouple used to calculate them. Sahai and Overfelt[9] reported significant variation in the calculated interface HTC (investment cast nickel) when the thermocouple position is varied by 0.5 mm. Although Sahai[20] also reported that mold thickness and thermal conductivity are significant factors.

The value of the external (mold/atmosphere) HTC (h_{ext}) used also affects the calculation of h_{int} (alloy/mold HTC). The sensitivity of h_{int} to uncertainty in the measurement of h_{ext} is shown in Figure 18. Here the value of h_{ext} is artificially valued by ±10 pct. This level of uncertainty does affect the calculation, but the trend in variation of h_{int} with temperature is not broken, and the inverse model does not become unstable. The effects are not surprising, given that h_{ext} essentially controls the departure of heat from the entire system under study.

Below 570 °C (the eutectic temperature), the effect of uncertainties is reduced. This is probably because the temperature difference across the interface increases significantly, and the heat flux at the interface drops as solidification is nearing completion. (The solid fraction of A356 increases rapidly at 570 °C). Also at this point, thermal gradients in the mold have flattened, which will make uncertainties in mold thermocouple position less important.

VI. CONCLUSIONS

Based on the preceding analysis, the following conclusions are drawn regarding the calculation of interface HTCs using the method described.

1. Experiments were performed involving the investment casting of aluminum alloys. The new inverse method was used to calculate the interface HTCs for both convex and concave interfaces.
2. All variables studied had effects upon the interface heat transfer, and some complex cross interactions between the effects of variables (*e.g.*, freezing range of alloy, metallostatic head, and mold preheat) were found. The main findings are summarized in Table VIII. These observations should be of value in assigning realistic boundary conditions in computer models of the casting process. The effect of shape is significant, with different thermal behavior observed at convex (alloy/mold) interface than at concave (alloy/core) interfaces.
3. The bias of the thermocouple in the mold and the accuracy to which its position can be determined have a reasonably significant effect on the calculated results, but, in this work, uncertainties in thermocouple reading and position are controlled such that excessive error in calculated HTC does not occur.
4. Inaccuracy in the measurement of the mold/atmosphere HTC (h_{ext}) does affect the calculation significantly, but the inverse model retains its stability. However, as h_{ext} is a measure of the total heat loss to the surroundings, such effects are expected.

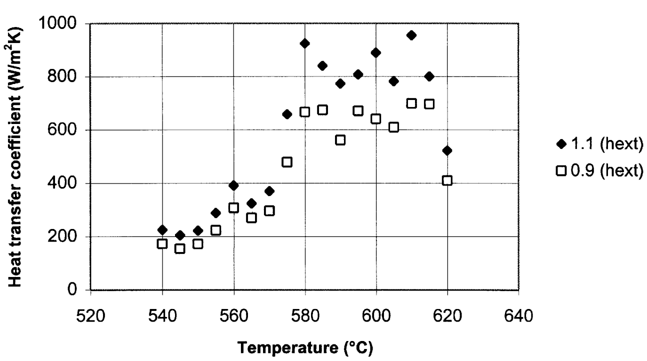

Fig. 18—Effect of uncertainty (±10 pct) in mold/atmosphere HTC on calculated internal HTC.

ACKNOWLEDGMENTS

The authors are grateful to Materials Ireland for the provision of support funding for this project. Thanks are also due to Mr. Nick Lumsden, for technical assistance in the UCD Solidification Laboratory.

APPENDIX A
Experimental details—mold/atmosphere HTC

Figure 19 shows a schematic of the cross section of the cylindrical test specimen used for the investigation of the mold/atmosphere HTC. This HTC needs to be quantified in order to later calculate the alloy/mold HTC.

A thick cylindrical alumino-silicate shell is built up around a ceramic core. Two thermocouple sites (T1 and T2) are incorporated into the shell, parallel to the central axis, during its manufacture. Each site consists of an alumina tube, of inside diameter 2 mm and outside diameter 3 mm, closed at one end. When the shell is complete, it is fired in a gas furnace at 1000 °C for 1 hour. Later 1 mm diameter thermocouples, type K, minerally insulated, stainless steel sheathed, are placed in the tubes. The shell is heated to 700

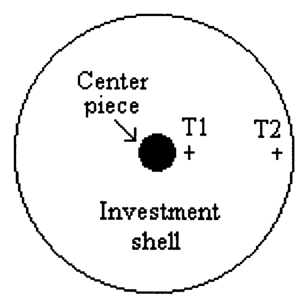

Fig. 19—Schematic of test for mold/atmosphere interface HTC estimation.

Table VIII. Results Summary

Alloy	Variables Which Affect Alloy/Mold HTC: Liquid Pressure	Mold Preheat	Mold Thickness	Alloy/Core HTC
413	Has little effect on mold/ alloy HTC	Large variation at low preheat. High preheat gives constant HTC	no significant effect on HTC	increases up to the liquidus and reduces continuously
A356	Significant factor, mold/ alloy HTC increases with depth	Same as 413. Also high preheat causes significant reduction in average HTC	Thicker mold significantly reduces HTC	increases to the liquidus, reduces suddenly, and increases slowly
319	Similar to A356 Significant at high mold preheat	Same as 413. No significant preheat effect for thick molds. High preheat increases sensitivity to head	Same as A356. Also for thin molds high preheat causes HTC to rise	Same as A356

°C and allowed to cool naturally. The temperatures at T1 and T2 are recorded at 2-second intervals. In order to determine the complete thermal history between T1 and the surface, the calculation is split into two parts. First, the thermal history between T1 and T2 is solved; this is a direct problem. Then, the thermal history between T2 and the surface is solved; this is an inverse problem. Next, the surface heat flux (q_s) in the radial (r) direction is calculated using Fourier's law (Eq. [2]). In which k is thermal conductivity. The HTC (h_{ext}) can then be calculated using Eq. [3], where T_s is the surface temperature, and T_{amb} is room temperature.

$$q_s = -k \left. \frac{\partial T}{\partial r} \right|_s \qquad [2]$$

$$h_{\text{ext}}\,(T_s) = \frac{q_s}{T_s - T_{\text{amb}}} \qquad [3]$$

APPENDIX B
Experimental details—alloy/mold HTC

The procedure starts with the manufacture of a cylinder of investment casting wax (the pattern). The pattern is first given a thin coat of zircon. It is dipped into a tank of zircon ceramic slurry and allowed to drain. Zircon stucco is then rained over the pattern, which is then left to dry. This procedure is repeated until the desired thickness of primary (zircon) shell has been built up. The pattern is then given a thicker (secondary) coat of alumino-silicate by the same method. When the shell has been built up to the required thickness and has been given sufficient time to dry, the wax is melted out. The shell mold is then fired in a gas furnace at 1100 °C for 1 hour.

One thermocouple site is placed in the wax pattern during its production. The other is placed in the shell during the manufacture of the mold. The sites are thin-walled (0.5 mm) alumina tubes, closed at one end, as per Appendix A. The tubes are carefully placed so that the closed ends of both are a distance, d, below the top of the casting, as illustrated in Figure 1. As per Tables II and III, $d = 8$ cm or $d = 12$ cm. More detail on this procedure can be found in Reference 11.

Prior to casting, the thermocouples, identical to those described in Appendix A, are placed in the tubes, which are located approximately 5 mm from the interface in the metal region and 2.5 mm from the interface in the mold region. The thermocouples are pushed down into the tubes as far as they will go, so that the sensing tips are also essentially at depth, d, below the free surface of the initially liquid alloy. The mold is then preheated in a small oven. When it has stabilized at the required temperature, it is removed and placed on kaowool insulation. Molten aluminum alloy is then poured into the mold at a temperature of approximately 700 °C to a height of 200 mm. In order to insulate the top of the casting, the pouring basin is filled with vermiculite. The temperature at the two thermocouple positions is recorded using a remote data logger.

Once the experiment has been completed, the casting and mold are sectioned to enable accurate measurement of the radial and axial positions of the thermocouple sensing tips.

REFERENCES

1. K.N. Prabhu, S.A. Kumar, and N. Venkataraman: *AFS Trans.*, 1994, vol. 102, pp. 827-32.
2. M. Krishnan and D.G.R. Sharma: *Scripta Metall. Mater.*, 1993, vol. 28, pp. 447-51.
3. F. Michael, P.R. Louchez, and F.H. Samuel: *AFS Trans.*, 1995, vol. 103, pp. 275-83.
4. T.G. Kim and Z.H. Lee: *Int. J. Heat Mass Transfer*, 1997, vol. 40 (15), pp. 3513-25.
5. G. Georgiev: *J. Mater. Sci. Technol.*, 1996, vol. 4 (2), pp. 39-48.
6. V. Hernandez, F. Decultieux, P. Schmidt, I. Svensson, and C. Levaillant *Iron Steel Inst. Jpn.*, 1995, vol. 35 (6), pp. 805-12.
7. J.C. Sturm and P.R. Sahm: in *Modeling of Casting, Welding, and Advanced Solidification Processes IV*, (A.F. Giamei and G.J. Abbaschian), eds., TMS, Warrendale, PA, 1988, pp. 69-71.
8. J.T. Anderson, G.T. Gethin, and R.W. Lewis: *Int. J. Cast Met. Res.*, 1997, vol. 9 (5), pp. 285-93.
9. V. Sahai and R.A. Overfelt: *AFS Trans.*, 1995, vol. 103, pp. 627-32.
10. D. O'Mahoney: Ph.D. Thesis, University College Dublin, Dublin, 2000.
11. D. O'Mahoney and D.J. Browne: *Exp. Thermal Fluid Sci.*, 2000, vol. 22 (3–4), pp. 111-22.
12. L. Bäckerud, G. Chai, and J. Tamminen: *Solidification Characteristics of Aluminum Alloys*, vol. 2, *Foundry Alloys*, AFS/Skanaluminium, Stockholm, 1991.
13. J.C. Escobedo, M.A. Ramirez, D.A. Cortés, A. Flores, A.H. Castillejos, and F.A. Acosta: *Light Metals 1997*, TMS, Warrrendale, PA, 1997, pp. 821-25.
14. D.J. Browne and K. Sayers: *Modeling of Casting, Welding, and Advanced Solidification Processes VII*, M. Cross and J. Campbell, eds., TMS, Warrendale, PA, 1995, pp. 441-48.
15. D.M. Grove and T.P. Davis: *Engineering Quality and Experimental Design*, Longman Scientific and Technical, Harlow, United Kingdom, 1992.
16. T.R. Thomas: *ASME J. Heat Transfer*, 1975, vol. 97 (2), pp. 305-07.
17. R.N. Smith and E. Meeks: *Expt. Thermal Fluid Sci.*, 1993, vol. 7, pp. 22-29.
18. F.L. Tan: *J. Mater. Proc. Sci.*, 1997, vol. 6, pp. 105-21.
19. J.M. Owen: *J. Mech. Eng. Sci.*, 1997, vol. 21 (3), pp. 323-31.
20. V. Sahai: *J. Thermophys. Heat Transfer*, 1998, vol. 12 (4), pp. 562-66.